

On chip cell separator using magnetic bead-based enrichment and depletion of various surface markers

Matthew D. Estes · Jaephil Do · Chong H. Ahn

Published online: 11 December 2008
© Springer Science + Business Media, LLC 2008

Abstract This paper presents an on-chip magnetic cell sorting system for the sorting of cells based on a variety of surface markers. A polymer lab on a chip integrated with an electroplated array of Ni/Fe permalloy has been designed, fabricated, and characterized for the separation of cell substitutes at a variety of flow rates and incubation times. The system sequentially labels cell substitutes with magnetic beads and sorts them, repeating this process to sort for a variety of surface markers. Flow rates and incubation times were varied to characterize the system and produce the best combination of high specific capture and low nonspecific capture. The separation system developed on polymer is selective and efficient while being low cost, portable, and fabricated in a modular structure that can be integrated with other cell handling processes.

Keywords Magnetic sorting · Enrichment and depletion of surface markers · Polymer · Microfluidics

1 Introduction

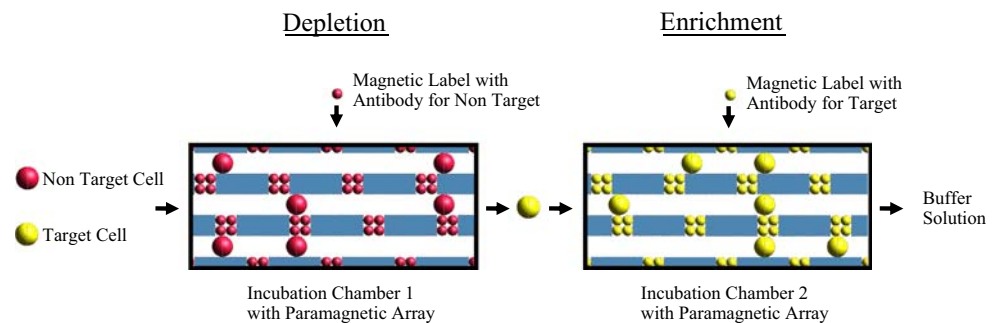
Recently there has been a large demand for the mapping of particular cellular functions to cellular subpopulations (Flynn et al. 2007; Kovarova et al. 2007). This mapping is frequently delineated by cell surface markers, with some markers being desired (positive selection) and others prohibited (negative selection) (De Rosa et al. 1993). As the marker requirements of a cellular subpopulation become more numerous and specific, the amount of these subpopulations present in a given sample begins to drop dramatically. Biological micro-electro-mechanical systems (BioMEMS) technology has been at the forefront of cell handling for small volumes of cells (Auroux et al. 2002; Edd et al. 2008) and proves to be an excellent format for work in this particular area.

The BioMEMS field, however, comes with its own limitations. On-chip magnetic cell sorting typically makes use of off-chip mixing and incubation of cells with their magnetic labels. Prior work has been done to combine binding and sorting functions for cells and labels on a single chip (Liu et al. 2007; Tan et al. 2005). To sort for multiple surface markers on a single device this will prove a necessity (Estes et al. 2007). Each time cells are removed from a sorting system to be handled on a macroscale between sorting runs as much as 70% of the cells are lost (Martin-Henao et al. 2001). A method must be devised to integrate multiple rounds of cell/marker incubation and subsequent sorting in a modular form on a single chip so that researchers can have access to highly specific cell subpopulations without concern for loss of these rare phenotypes. This paper presents an integrated on-chip cell sorting system capable of both positive and negative cell substitute selection on a single chip. The device is outlined in the block diagram presented in Fig. 1.

M. D. Estes (✉) · C. H. Ahn
Department of Biomedical Engineering,
MicroSystems and BioMEMS Lab, University of Cincinnati,
814 Rhodes Hall,
Cincinnati, OH 45221, USA
e-mail: estesmd@email.uc.edu

J. Do · C. H. Ahn
Department of Electrical and Computer Engineering,
MicroSystems and BioMEMS Lab, University of Cincinnati,
814 Rhodes Hall,
Cincinnati, OH 45221, USA

Fig. 1 Block diagram of serial magnetic cell sorting system



2 Principle and design

The two key subunits required for this device to function properly are a means of introducing and incubating cell substitutes with their magnetic labels to facilitate binding and a magnetic separator to separate labeled cells from unlabeled ones.

For the purpose of mixing cell substitutes and magnetic beads, a variety of mixer designs making use of passive mixing were considered, including rotation-based mixers (Park et al. 2004), laminating mixers (Kim et al. 2006), and Tesla structure mixers (Hong et al. 2004). All of these designs have been found to provide good mixing at a variety of flow rates, but ultimately a simple sedimentation design was decided on as a means of introducing cell substitutes with their magnetic labels. This stems out of prior experience indicating that a low flow rate is necessary to allow enough time for strong antibody binding, but if magnetic beads are pumped through a large magnetic field at a low flow rate blockage typically becomes a significant problem. The solution to this problem is to pump through magnetic beads in the absence of an applied magnetic field to effect good dispersion of magnetic beads throughout the sorting chamber. This can be followed by the application of a strong magnetic field and the introduction of cell substitutes to the sorting chamber where they are incubated for a time to allow binding. The cell substitutes settle to the bottom of the chamber in a few minutes where an incubation time on the order of one hour provides sufficient time for them to bind to their complimentary magnetic beads. This system avoids the clogging of magnetic beads at low flow rates while at the same time giving the cell substitutes a high incubation time to allow good binding.

A separation mechanism was needed to capture the cell substitutes once they were labeled. A magnetic immobilization separation scheme was decided on due to its simplicity, low cost, and ease of fabrication and miniaturization (Choi et al. 2000, 2002). By sequentially immobilizing magnetic beads and incubating cell substitutes, the researcher can perform multiple rounds of separation without removing the cell substitutes to the macro world for a second set of mixing and incubation. This provides a

significant advantage over flow through deflection based magnetically actuated cell sorters (Pamme 2007). Within this category, paramagnetic array separation was selected because of its ability to capture a wide dispersion of magnetic beads, without the power source needed by electromagnetic separators (Lee et al. 2006). This provides a large area for subsequent cell substitute capture while at the same time avoiding the large bead aggregates produced by bulk magnetic separators that can easily clog a microchannel (Do and Ahn 2008). Paramagnetic arrays in the past have occasionally suffered from low percentage yields of magnetic beads and researchers have been content merely to show the capture of beads as a measure of success (Choi et al. 2001; Ahn et al. 1996). For this reason in the present work large serpentine microchannels were used, measuring 1,000 μm wide and allowing for a large capture area to ensure high bead and cell substitute retention. The relatively large channel size also allows for working with sample sizes in the range of hundreds of microliters so that a large number of cell substitutes can be sorted simultaneously. The overall system design and sorting procedure is outlined in Fig. 2.

The magnetic force imparted to the magnetic beads can be characterized using the following equation:

$$F = (1 - N_d)\mu_0\mu_r V_p (H \cdot \nabla H)$$

where F is the force on a magnetic bead in a particular direction, N_d is the demagnetizing factor, μ_0 is the permeability in a vacuum, μ_r is the relative permeability, V_p is the volume of the bead, and H is the applied magnetic field. Increasing the magnetic field gradient will cause an increase in the magnetic force applied to a bead. Producing a strong magnetic field gradient over a large area can prove difficult, and it is easier to use micropatterned materials of varying magnetic saturation levels to repeatedly generate small areas of high field gradient, creating localized perturbations in a larger otherwise uniform magnetic field. A micro paramagnetic array on the order of the beads themselves can create local spikes in the magnetic field gradient that result in strong and predictable bead immobilization.

Computer simulation for the device was carried out using MagNet software from Infolytica Corporation. With

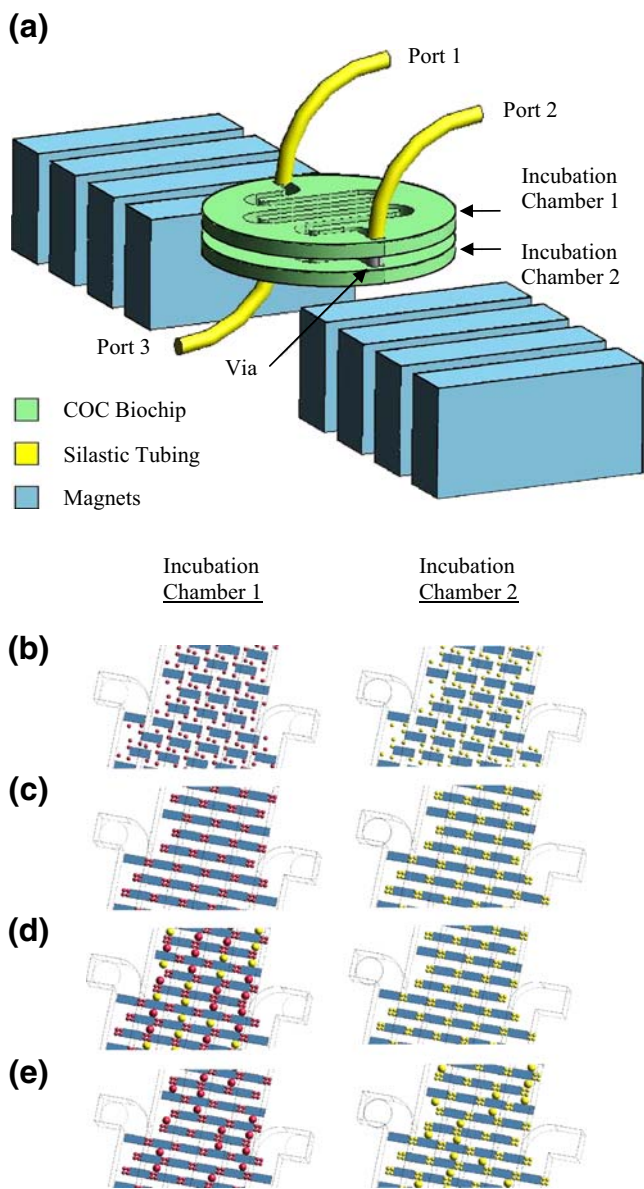


Fig. 2 Schematic illustration of serial on-chip magnetic cell sorting system (not to scale): **(a)** Overall system architecture; **(b)** introduction of magnetic beads into both Incubation Chambers; **(c)** immobilization of the magnetic beads by use of external magnetic field; **(d)** introduction of mixed cell substitute population into Incubation Chamber 1 and incubation; and **(e)** rinsing unbound cell substitutes from Incubation Chamber 1 into Incubation Chamber 2, and incubating, followed by a second rinsing step

20×50×1 μm paramagnetic elements composed of 70% nickel and 30% iron spaced at a distance of 20 μm and an applied magnetic flux density of 0.4 T, the magnetic flux density throughout the paramagnetic array was attained as shown in Fig. 3. Analyzing this data indicates that between the paramagnetic elements an increased flux density of 0.75 T was attained, while the flux density in regions a mere 20 μm away was reduced to 0.35 T. This results in the creation of small areas with a gradient of 0.4 T/20 μm

repeating throughout the entire paramagnetic array. This is responsible for the dispersed magnetic bead capture seen later that facilitates a wide area of cell substitute capture.

With the considerations for the system components and simulation results, an on-chip magnetic cell sorting device is designed as shown in Fig. 2. The paramagnetic arrays are 20 μm by 50 μm across and 1 μm thick with 20 μm of spacing. The microchannels are 1,000 μm across and 500 μm high. The device makes use of separate flowing of magnetic beads and cell substitutes into a long microchannel for separation. Sedimentation of the beads is used so that complex mixing is not required and the agent of capture is the dispersed paramagnetic array.

3 Fabrication

The magnetic cell sorting device was fabricated using cyclic olefin copolymer (COC) wafers for creating the microfluidic channels and housing the paramagnetic arrays. COC was chosen because of its well characterized performance for lab-on-a-chip devices (Hong et al. 2003). The fabrication procedure is outlined in Fig. 4.

The microfluidic channels were fabricating starting with an RCA cleaned 3 in. nickel disk. Using Omnicot adhesion promoter, SU8-2075 Photoresist (PR) was deposited on the wafer. The PR was pre-exposure baked, exposed to a dose of 250 mJ/cm² of ultraviolet light, and post-exposure baked. The PR was developed in propylene glycol methyl ether acetate, and the wafer was treated with oxygen plasma to remove residual PR. The remaining PR was used as a mask to guide nickel electroplating of channels 1,000 μm wide with 500 μm spacing. The PR was then completely removed using MicroChem PG Remover and oxygen plasma treating (Puntambekar et al. 2002). The electroplated nickel served as a master mold for fabricating

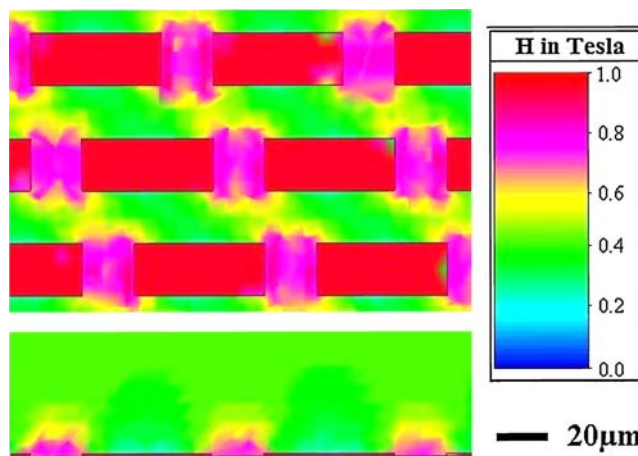


Fig. 3 Simulated magnetic flux density around the paramagnetic array using MagNet software

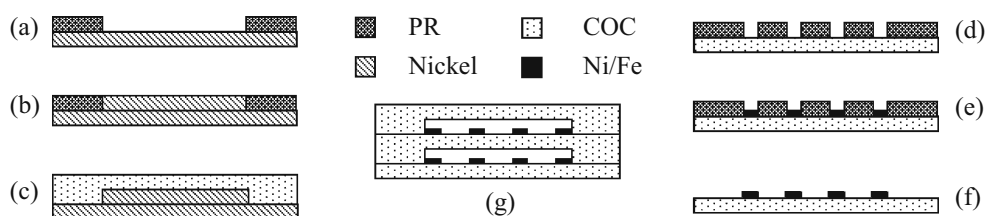


Fig. 4 Summary of fabrication procedure: (a) Photoresist patterning; (b) nickel electroplating; (c) injection molding; (d) photoresist patterning; (e) nickel/iron electroplating; (f) photoresist removal; and (g) thermoplastic fusion bonding to create the final device

patterned Zeonor COC wafers using a BOY 22A precision injection molding machine (Kim et al. 2006). Each COC wafer can be made cheaply in about a minute (Ahn et al. 2004).

Next the paramagnetic arrays for capture of the magnetic beads had to be fabricated. These were made starting with blank COC wafers. Since COC is a natural insulator, the wafers were coated with an adhesion layer of titanium and a seed layer of copper to facilitate subsequent electroplating. Shipley 1818 PR was deposited onto the wafers, baked, exposed, and patterned using MP351 developer. The Ni/Fe paramagnetic array was electroplated onto the wafers and the PR was removed using acetone. The copper and titanium layers were removed and the paramagnetic array was then embossed into the surface of the wafer to reduce surface roughness. At this point the second wafer containing the paramagnetic array was complete and ready for assimilation with the rest of the device.

The two wafers were bonded together using an MTP-10 hot embossing machine to facilitate high strength thermoplastic fusion bonding. The embossing machine was programmed to provide 0.4 kg of force at a temperature of 128°C for 20 min.

After bonding the device was prepared for integration with macro scale syringe pumps by the insertion of 0.79 in. external diameter 1575 PEEK tubing from Upchurch Scientific into the fluidic contact holes. A tight seal was attained by treating the point of contact with Loctite 3211 light cure adhesive and exposing to UV light for 1 min. The PEEK tubing is interfaced with soft flexible Silastic silicone laboratory tubing from Dow Corning that has an internal diameter of 0.64 mm. This soft tubing fit snugly over the PEEK tubing creating a tight seal without the need for adhesive. The soft tubing also fit snugly over a standard 5 ml syringe needle used with a Harvard Apparatus Syringe Pump 33 interfaced with LabVIEW software to provide precise fluidic control. The completed device is shown in Fig. 5.

Before experimentation began the microchannels were filled with dye and examined under a microscope to ensure all channels are open and all bonding is tight. The microchannels are then rinsed with phosphate buffered saline (PBS) for 5 min, treated with a 100% concentration

of Starting Block Protein Blocking Solution from Pierce Biotechnologies for 1 h on each side, rinsed with air for 1 min, rinsed with PBS for 1 min, and then dried with Nitrogen for 1 min. This surface treatment is performed to prevent nonspecific adhesion of biological molecules.

Strong external neodymium magnets 0.5 in. in thickness by 1 in. by 2 in. magnetized through their thickness were procured for subsequent use with the device from K&J Magnetics, Inc. When four of these magnets are placed on either side of the incubation chambers for a total of eight magnets with a central spacing of 3 in., they provide a magnetic field of 0.4 T with a local field gradient intensified by the paramagnetic array, shown in Fig. 6(a).

4 Experimental procedure

The experimental procedure was carried out as follows using polystyrene cell substitutes coated in a specific biomolecule, magnetic beads labeled with a biomolecule complimentary to that of the cell substitutes, and a variety of flow rates and incubation times. All cell substitutes and magnetic beads were purchased from Spherotech, Inc. Two micrometer diameter magnetic beads coated with streptavidin for Magnetic Chamber 1 were first pumped through the device at a rate of 20 $\mu\text{L}/\text{min}$ using Port 1 at a concentration of 0.5 $\mu\text{g}/\mu\text{L}$. The external magnets were

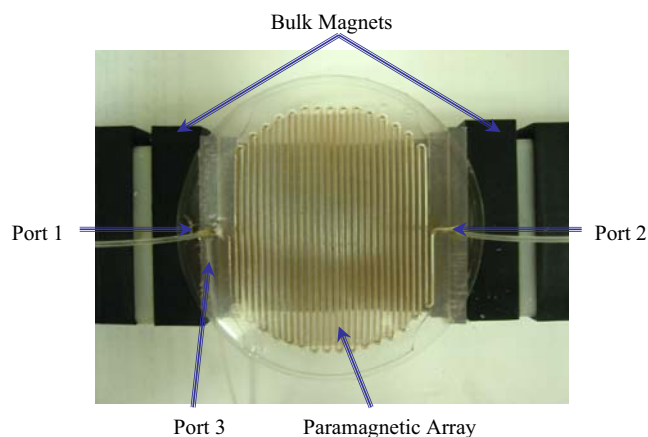


Fig. 5 Photograph of fabricated device

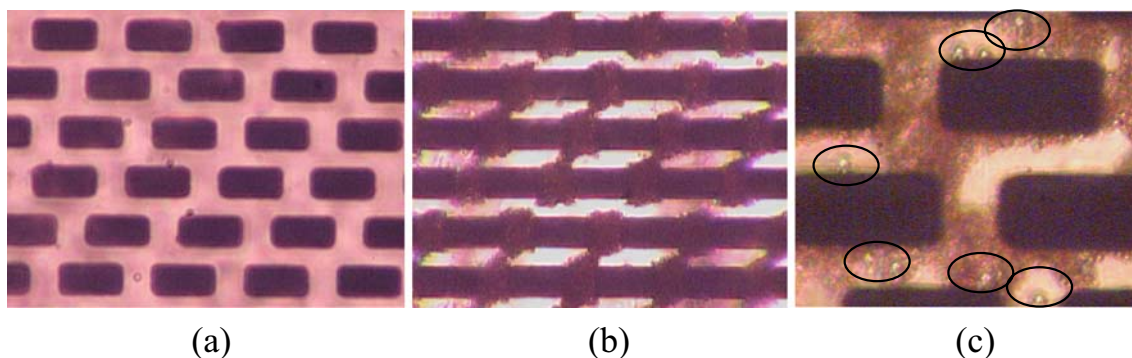


Fig. 6 Micrographs of (a) fabricated paramagnetic array; (b) selectively immobilized magnetic beads on the paramagnetic array; and (c) captured cell substitutes (circled in black). Black paramagnetic elements are 50 by 20 μm in size

then applied underneath the device on either side of the magnetic chamber. This quickly immobilized the beads on the bottom of the microchannel, evenly dispersing them throughout the magnetic chamber by use of the distributed magnetic field gradients generated by the permalloy structures. This can be seen in Fig. 6(b). The microchannel was then rinsed with Nitrogen for 1 min at 20 $\mu\text{L}/\text{min}$, buffer solution for 5 min at 20 $\mu\text{L}/\text{min}$, and again Nitrogen at 20 $\mu\text{L}/\text{min}$ for as much time as was needed to clear the channel. At this point the device was ready for one step sorting of the cell substitutes in Magnetic Chamber 1.

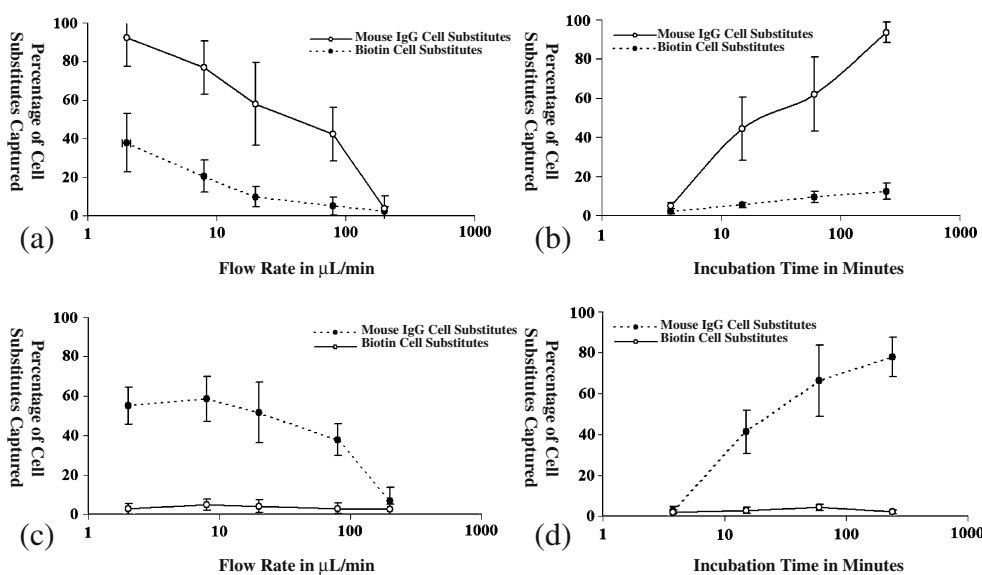
A mixed population of 0.25 $\mu\text{g}/\mu\text{L}$ 5 μm biotin coated cell substitutes and 0.25 $\mu\text{g}/\mu\text{L}$ non-fluorescent Mouse IgG coated cell substitutes in 250 μL of phosphate buffered saline solution was pumped into Magnetic Chamber 1. This was incubated for one hour and then pumped out of the micro chamber (Ekins 1998). These cell substitutes can be seen in Fig. 6(c). With a total volume of 500 μL , the duration of this rinsing step was varied based on the speed to give as much as time as was needed to completely rinse

out the channel and can be calculated as the incubation chamber volume divided by the volumetric flow rate.

To characterize the effect of incubation time on cell retention rates, experiments were carried out using a set flow rate of 20 $\mu\text{L}/\text{min}$ and the incubation time was varied. The basic procedure outlined above was repeated but with incubation times of 3 min 45 s, 15 min, 1 h and 4 h.

Once the data these steps provided was analyzed and the knowledge of the effects of flow rate and incubation time on capture rates was known, it was possible to move forward to proper two step sequential separation. For this phase of the study Magnetic Chamber 1 was prepared as described above with streptavidin labeled magnetic microbeads. Magnetic Chamber 2 was similarly prepared with a 0.5 $\mu\text{g}/\mu\text{L}$ solution of 2 μm magnetic beads coated with anti-Mouse IgG. Then following the above procedure, 250 μL of buffer containing 0.25 $\mu\text{g}/\mu\text{L}$ fluorescent 5 μm biotin coated cell substitutes and 0.25 $\mu\text{g}/\mu\text{L}$ non-fluorescent Mouse IgG coated cell substitutes was pumped into Magnetic Chamber 1. Following an incubation time of 1 h,

Fig. 7 Characterization result of captured cell substitutes in (a) Incubation Chamber 1 with respect to flow rate, (b) Incubation Chamber 1 with respect to incubation time, (c) Incubation Chamber 2 with respect to flow rate, and (d) Incubation Chamber 2 with respect to incubation time



Magnetic Chamber 1 is flushed out with buffer at a flow rate of 20 $\mu\text{L}/\text{min}$ for 25 min so that all unbound cell substitutes are displaced into Magnetic Chamber 2. They are incubated a second time for 1 h and then flushed out with buffer at a flow rate of 20 $\mu\text{L}/\text{min}$ for 25 min so that unbound cell substitutes are removed from the system.

5 Results and discussion

The immobilized cell substitutes were then assessed for their rates of capture in Incubation Chamber 1 at various flow rates and incubation times. The work examining the rate of specific capture of biotin labeled cell substitutes in Incubation Chamber 1 is presented in Fig. 7(a). As can be seen, increasing the flow rate during the rinsing step decreases both the amount of specific and nonspecific cell substitute immobilization. At a low flow rate there is excellent specific cell substitute immobilization, approaching 100%, but the degree of nonspecific capture is prohibitively high, at almost 40%. At the maximum flow rate tested of 200 $\mu\text{L}/\text{min}$ nearly all cell substitutes, whether specific or nonspecific, are removed. The flow rate of 20 $\mu\text{L}/\text{min}$ was ultimately selected as the best option due to its combining a relatively high specific cell yield of 60% with a nonspecific cell capture rate of roughly 10%.

The effect of the incubation time on cell substitute capture was examined using this flow rate of 20 $\mu\text{L}/\text{min}$. The varying incubation times probed are given in Fig. 7(b). Given an incubation time of a few minutes, the degree of specific cell substitute capture does not rise much above the nonspecific baseline. At 15 min there is a noticeable increase in specific cell substitute capture and this increases with time up to the maximum time of 4 h tested. This is due to more time increasing the chance of a cell substitute contacting a matching magnetic bead and the more time the two are present together the stronger the molecular bonding is between them.

The next step of this work was to examine specific capture of Mouse IgG labeled cell substitutes by anti-Mouse IgG labeled magnetic beads in Incubation Chamber 2, once they had already passed through Incubation Chamber 1. This data is presented in Fig. 7(c) and (d). Similar effects of flow rate and incubation time are seen compared to what was experienced with the biotin labeled cell substitutes. Increasing flow rate decreases the amount of cell substitutes captured. Increasing incubation time increases the amount of cell substitutes captured but at the expense of an increased process time. There is less overall cell substitute capture in Incubation Chamber 2 and this is a result of a reduction in the number of available cell substitutes after the first round of capture in Incubation Chamber 1.

6 Conclusion

This paper has shown for the first time serial magnetic separation for multiple surface markers on a single chip. Joining of cell substitutes and magnetic labels was accomplished by means of sedimentation. Separation was accomplished via an electroplated array of Ni/Fe permalloy. The device was characterized at a variety of flow rates and incubation times. Flow rates in the 8–80 $\mu\text{L}/\text{min}$ range have been found to produce the best combination of high specific capture and low nonspecific capture. Incubation for 4 h produces the best possible capture of specific cell substitutes and low retention of nonspecific cell substitutes. Incubation for 1 h was also deemed acceptable, because although it offers a lower yield it greatly improves the process time. Overall this device is significantly cheaper to manufacturer than its macroscale counterparts and can easily be integrated with other micro total analysis system components.

References

- C.H. Ahn, M.G. Allen, W. Trimmer, Y.J. Jun, S. Erramilli, *IEEE K. Microelectromech. Syst.* **5**, 151–158 (1996). doi:10.1109/84.536621
- C.H. Ahn, J.W. Choi, G. Beaucage, J.H. Nevin, J.B. Lee, A. Puntambekar, J.Y. Lee, *Proc. IEEE* **92**, 154–173 (2004). doi:10.1109/JPROC.2003.820548
- P.A. Auroux, D. Iossifidis, D.R. Reyes, A. Manz, *Anal. Chem.* **74**, 2637–2652 (2002). doi:10.1021/ac020239t
- J.W. Choi, C.H. Ahn, S. Bhansali, H.T. Henderson, *Sens. Actuators* **68**, 34–39 (2000). doi:10.1016/S0925-4005(00)00458-5
- J.W. Choi, K.W. Oh, A. Han, N. Okulan, C.A. Wijayawardhana, C. Lannes, S. Bhansali, K.T. Schlueter, W.R. Heineman, H.B. Halsall, J.H. Nevin, A.J. Helmicki, H.T. Henderson, C.H. Ahn, *Biomed. Microdevices* **3**, 191–200 (2001). doi:10.1023/A:1011490627871
- J.W. Choi, K.W. Oh, J.H. Thomas, W.R. Heineman, H.B. Halsall, J.H. Nevin, A.J. Helmicki, H.T. Henderson, C.H. Ahn, *Lab Chip* **2**, 27–30 (2002). doi:10.1039/b107540n
- L. De Rosa, A. Montuoro, A. Pandolfi, U. Paladini, T. Lanti, R. Morara, A. De Laurenzi, *Int. J. Artif. Organs* **5**, 102–107 (1993)
- J. Do, C.H. Ahn, *Lab Chip* **8**, 542–549 (2008). doi:10.1039/b715569g
- J.F. Edd, D. Di Carlo, K.J. Humphry, S. Koster, D. Irimia, D.A. Weitz, M. Toner, *Lab Chip* **8**, 1262–1264 (2008). doi:10.1039/b805456h
- R.P. Ekins, *Clin. Chem.* **44**, 2015–2030 (1998)
- M.D. Estes, J. Do, C.H. Ahn, *Proceedings of the 11th International Conference on Micro Total Analysis Systems (micro-TAS 2007)*, 1420–1422 (2007)
- A. Flynn, F. Barry, T. O'Brien, *Cytotherapy* **9**, 717–726 (2007). doi:10.1080/14653240701584578
- C.C. Hong, S. Murugesan, S. Kim, G. Beaucage, J.W. Choi, C.H. Ahn, *Lab Chip* **3**, 281–286 (2003). doi:10.1039/b306116g
- C.C. Hong, J.W. Choi, C.H. Ahn, *Lab Chip* **4**, 109–113 (2004). doi:10.1039/b305892a
- D.S. Kim, S.H. Lee, C.H. Ahn, J.Y. Lee, T.H. Kwon, *Lab Chip* **6**, 794–802 (2006). doi:10.1039/b516495h
- L. Kovarova, T. Buchler, L. Pour, L. Zahradova, D. Ocadlikova, A. Svobodnik, M. Penka, J. Vorlicek, R. Hajek, *Neoplasma* **54**, 297–303 (2007)

- H. Lee, Y. Liu, R.M. Westervelt, D. Ham, *IEEE J. Solid State Circuit* **41**, 1471–1480 (2006). doi:[10.1109/JSSC.2006.874331](https://doi.org/10.1109/JSSC.2006.874331)
- Y.J. Liu, S.S. Guo, Z.L. Zhang, W.H. Huang, D. Baigl, M. Xie, Y. Chen, D.W. Pang, *Electrophoresis* **48**, 4713–4722 (2007). doi:[10.1002/elps.200700212](https://doi.org/10.1002/elps.200700212)
- G.A. Martin-Henao, M. Picon, B. Amill, S. Querol, C. Ferra, A. Granena, J. Garcia, *Bone Marrow Transplant.* **27**, 683–687 (2001). doi:[10.1038/sj.bmt.1702860](https://doi.org/10.1038/sj.bmt.1702860)
- N. Pamme, *Lab Chip* **7**, 1644–1659 (2007). doi:[10.1039/b712784g](https://doi.org/10.1039/b712784g)
- S.J. Park, J.K. Kim, J. Park, S. Chung, C. Chung, J.K. Chang, J. *Micromech. Microeng.* **14**, 6–14 (2004). doi:[10.1088/0960-1317/14/1/302](https://doi.org/10.1088/0960-1317/14/1/302)
- A. Puntambekar, S. Murugesan, R. Trichur, H. Cho, S. Kim, J.W. Choi, C.H. Ahn, *Proceedings of the 6th International Conference on Micro Total Analysis Systems (micro-TAS 2002)*, 425–442 (2002)
- W.H. Tan, Y. Suzuki, N. Kasagi, N. Shikazono, K. Furukawa, T. Ushida, *JSME Int. J. Ser. C* **48**, 425–435 (2005)